Different Effects of Tri(acryloyloxyethyl) Phosphate on the Thermal Degradation of Photopolymerized Epoxy Acrylate and Polyurethane Acrylate Films

Hongbo Liang, Zhanguang Huang, Wenfang Shi

State Key Laboratory of Fire Science and Department of Polymer Science and Engineering, University of Science and Technology of China, Hefei, Anhui 230026, People's Republic of China

Received 14 March 2005; accepted 24 July 2005
DOI 10.1002/app.22751
Published online in Wiley InterScience (www.interscience.wiley.com).

ABSTRACT: Tri(acryloyloxyethyl) phosphate (TAEP) was blended in different ratios with epoxy acrylate EB600 and polyurethane acrylate EB270 to obtain a series of UV curable flame retardant resins. The thermal degradation mechanisms of their cured films in air were studied by thermogravimetric analysis, *in situ* Fourier-transform infrared spectroscopy, and direct pyrolysis/mass spectrometry measurements. The results showed that the phosphate group in TAEP first degraded to form poly(phosphoric acid) before the degradation of EB600. Then, the formed poly(phosphoric acid) effectively promoted the conversion of EB600 to form char, which prevented the sample from further burning. However, urethane group in EB270 degraded simultaneously with phosphate group in TAEP, leading to not effectively increase the conversion of EB270 to char during the thermal degradation. It was thus found that the addition of TAEP more effectively improved the thermal stability, flame retardance, and the char yield during combustion of EB600 than those of EB270. © 2006 Wiley Periodicals, Inc. J Appl Polym Sci 99: 3130–3137, 2006

Key words: flame retardance; multifunctional phosphate acrylate oligomer; photopolymerization; degradation

INTRODUCTION

UV-radiation curing has become a well-accepted technology in the fields of fast-drying protective coatings, electronics, inks, and additives because of its high cured speed, energy conservation, pollution reduction, and cost-effectiveness.[1,2] However, the cured films of conventional UV curable resins are flammable, which demands the development of flame retardant (FR) systems to reduce fire hazards for some applications, such as the matrix for optical fibers[3] and FR wood coatings.[4]

The phosphorus-containing monomers and oligomers used as FRs for UV curable systems have drawn much attention.[5–7] These FR materials overcome several drawbacks associated with physical blends and halogen-type FRs.[8–10] The effect of phosphorus-containing FR was proposed to be via a solid-phase mechanism.[11,12] The phosphorus moiety confers flame retardancy mainly by modifying the mode of thermal decomposition of the basic ignition,[13] which determines the efficiency of FR on the basic ignition. In our previous work, a phosphorus-containing monomer, tri(acryloyloxyethyl) phosphate (TAEP), was synthesized, possessing the limiting oxygen index (LOI) value of 36.[14] It has been used as reactive-type FR monomer together with commercial epoxy acrylate and polyurethane acrylate oligomers. The results have shown that the flame retardance of the cured films could be improved with TAEP addition.[15] Moreover, in comparison with EB270, the thermal stability of EB600 with TAEP addition is more significant. This indicates that TAEP is more effective to improve the flame retardance of EB600 than that of EB270. It is, therefore, necessary to study the different effects of TAEP in the thermal decomposition of the basic EB270 and EB600.

In this study, TAEP was blended with EB270 and EB600 in different ratios to obtain UV curable FR resins. The FR property of the cured films was studied by the LOI. The chemical structure changes during the thermal degradation of the films were monitored by *in situ* Fourier-transform infrared spectroscopy (FTIR). The structures of pyrolysis products from the thermal decomposition were determined by direct pyrolysis/mass spectrometry (DP–MS) analysis, and allowed a detailed description of the thermal degradation pathways and on the reactions, leading to the formation of charred residues.

EXPERIMENTAL

Materials

EB600, an epoxy acrylate with a molar mass of 500 g mol^{-1}, and EB270, an aliphatic polyurethane acrylate

Correspondence to: W. Shi (wfshi@ustc.edu).
Contract grant sponsor: China NKBRSF Project; contract grant number: 2001CB409600.

TABLE I
Flammability and CYs of EB600, EB270, TAEP, and Their Blends

Resin	Flammability		CY (%)
	LOI	UL-94	
EB600	21	Fail	5
EB600–0.I7TAEP	26	Fail	15.2
EB600–0.25TAEP	27.3	Fail	27.3
EB600–0.33TAEP	28.3	V_1	38.4
EB600–0.50TAEP	31.5	V_0	45.5
EB270	19.5	Fail	0
EB270–0.I7TAEP	22	Fail	3.0
EB270–0.25TAEP	23	Fail	7.0
EB270–0.33TAEP	25.2	Fail	14.8
EB270–0.50TAEP	26	Fail	20.5
TAEP	36	V_0	28.7

with a molar mass of 1500 g mol^{-1}, were supplied by UCB, Belgium. TAEP, with unsaturation concentration of 7.65 mmol g^{-1}, was synthesized by the reaction of phosphorus oxychloride with hydroxylethyl acrylate, which was described by author elsewhere.[14] 2-Hydroxy-2-methyl-1-phenyl-1-propanone (Darocur 1173), supplied by Ciba-Geigy, Switzerland, was used as a photoinitiator.

Sample preparation

The formulations with 2 wt % Darocur 1173 addition were stirred for 20 min at 60°C, then UV-cured with a UV irradiation equipment (80 W cm^{-1}; Lantian, Beijing) to obtain homogenous films. The compositions of formulations are listed in Table I.

Measurements

The thermogravimetric analysis (TGA) was carried out on a Shimadzu TG-50 apparatus, using a heating rate of 10°C min^{-1} in air. Concerning the thermal analyses of EB600/TAEP and EB270/TAEP formulations, the curves of weight difference between the experimental and theoretical TG curves were computed.[16] The theoretical TG curve was computed by linear combination between the TG curves of resins and monomer. $W_{th}(T)_{[oligomer/monomer]} = xW_{exp}(T)_{oligomer} + yW_{exp}(T)_{monomer}$; $x + y = 1$. Where, $W_{exp}(T)_{oligomer}$ is the TG curves of the UV-cured pure commercial oligomer(EB600 and EB270) films; $W_{exp}(T)_{monomer}$ is the TG curves of the UV-cured pure TAEP film; and x and y are the weight percentages of oligomers and monomer in the blends, respectively. Then the curves of weight difference were given as, $\Delta(Weight)_{[oligomer/monomer]} = W_{exp}(T)_{[oligomer/monomer]} - W_{th}(T)_{[oligomer/monomer]}$, where $W_{exp}(T)_{[oligomer/monomer]}$is the TG curves of UV-cured oligomer/monomer blend films.

The Δ(Weight) curves allow the observation of eventual increases or decreases in the thermal stability of formulations compared to the combination of components analyzed separately.

The LOI values of cured films were measured using a ZRY-type instrument (China) on the sheets of 120 × 6 × 3 mm^3, according to ASTM D2863–77.

The *in situ* FTIR spectra were recorded with a Nicolet MAGNA-IR 750 spectrometer. The *in situ* FTIR data were measured using KBr disk method, in which the sample powder was dispersed in KBr powder, with a heating rate of 2°C min^{-1} in the range of 30–430°C.

DP–MS analysis was carried out with a Micromass gas chromatography-mass spectrometry (GCT-MS) spectrometer using the standard direct insertion probe for solid polymer materials, at a heating rate of 10°C min^{-1} in the range of 30–550°C. The mass data were continuously acquired at a scan rate of 0.1 s. Electron impact (EI) was used for the mass spectra with 70 eV and the mass range of 10–1000 *m/z*.

The combustion analysis was conducted with a ZRY-type instrument at the oxygen concentration of LOI measurements on the sheets of 120 × 6 × 3 mm^3. The sample before the burning and the char formed during burning were carefully weighed. The char yield (CY) was calculated by the following formula.

$$CY = (\text{char weight}/\text{weight of burned specimen}) \times 100$$

$$\text{Weight of burned specimen} = \text{total weight of the specimen} - \text{weight of unburned specimen}$$

RESULTS AND DISCUSSION

Thermal degradation behavior

The thermal stability of a polymeric material is very important when used as a FR, which mainly concerns the release of decomposition products and the formation of a char. The influence of TAEP on the thermal stability of EB600 and EB270 has been studied in our previous work.[15] The results showed that the thermal stability of UV cured EB270 and EB600 were improved by loading of TAEP. However, in comparison with EB270, the influence of TAEP on the thermal stability of EB600 was more significant. To investigate this difference between two oligomers, the weight difference curves of EB270 and EB600 with TAEP addition were calculated by the approach described in the aforementioned section.

Figure 1 shows the weight difference curves of EB600 with different TAEP contents. The weight loss difference curves for UV-cured EB600–0.33TAEP and

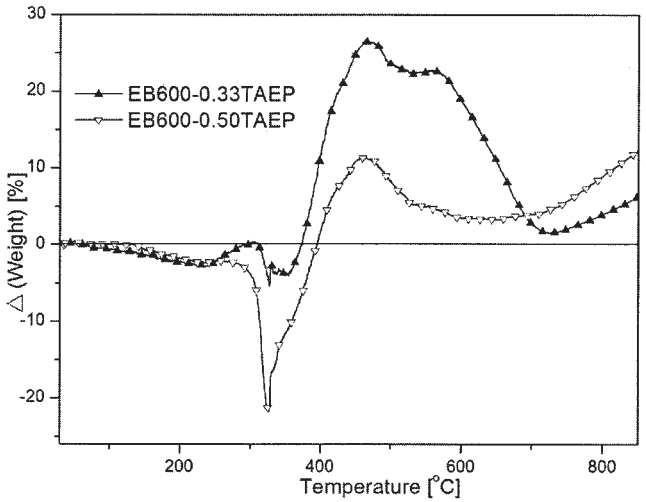

Figure 1 Weight difference curves for EB600/TAEP blends.

EB600–0.50TAEP show a large negative temperature range about 330°C. This is because the poly(phosphoric acid), which is the product from degradation of phosphates in TAEP before 270°C and has been found during DP–MS measurements in our previous work,[14] catalyzed the degradation of EB600, leading to the development of an intumescent system. Both the samples are stabilized over 400°C, with an important quantity of thermally stable char produced from the reactions between the decomposition products of EB600 and TAEP. Moreover, EB600–0.33TAEP sample shows a larger stabilization peak (about 25%) than that of EB600–0.50TAEP sample (about 10%) over 400°C. This also indicates that there have interactions between the degradation products of EB600 and TAEP.

Figure 2 shows the weight difference curves of EB270 with different TAEP contents. The weight loss difference curves for both UV-cured EB270–0.33TAEP and EB270–0.50TAEP show only one large negative peak about 320°C. The negative peak can be attributed to that poly(phosphoric acid), the product from degradation of phosphates in TAEP, catalyzed the degradation of EB270, leading to the development of an intumescent system. Indeed, the intumescent system can be observed by treating the cured films in a muffle furnace. Then, the UV-cured samples are stabilized over 400°C with very small stabilization char (about 5%).

From the comparison of Figure 1 with Figure 2, the UV-cured EB600 samples with TAEP addition have smaller destabilization peaks and larger stabilization peaks than those of EB270 samples with TAEP addition. This indicates that TAEP is more effective to develop char about 400°C for EB600 than EB270. The chemical structure changes during the degradation process were further studied by the *in situ* FTIR and DP–MS measurements.

Flame retardance

The LOI and UL-94 tests are widely used to evaluate the FR properties of materials and to screen FR formulations. The LOI and UL-94 data of the samples are listed in Table I. It can be seen that the LOI values increase with increasing TAEP content in both the resins. Moreover, TAEP is more effective to increase the LOI for EB600 than for EB270. This is consistent with their thermal behaviors. EB600 film with 50% TAEP addition reaches V_0 grade in UL-94 test, resulting from the higher efficiency of TAEP to develop char about 400°C for EB600 than EB270.

Phosphorus-containing compounds are a family of condensed-phase FRs, which are able to increase the conversion of organic matter to char during burning, and thus decrease the amount of flammable volatile gases reaching the flame zone, and reduce the heat transfer from the flame to the material. Thus, the CY during combustion is very important for a phosphorus-containing FR material. The CYs of all samples were measured and are also listed in Table I, respectively. The CY value increases from 0 for pure EB270 to 14.8 for EB270–0.33TAEP and then increases to 20.5 for EB270–0.50TAEP, while the CY value increases from 5 for pure EB600 to 38.4 for EB600–0.33TAEP and then increases to 45.5 for EB600–0.50TAEP. The enhancement of CY with TAEP addition can greatly decrease the amount of flammable volatile gases and thus improve the flame retardance. Moreover, EB600/TAEP blends have higher CYs during combustion than EB270/TAEP blends, and even higher than pure TAEP. This also indicates that the degradation products, poly(phosphoric acid), of TAEP can more effectively catalyze the degradation of EB600 to form char, which will be further studied by the following *in situ* FTIR and DP–MS measurements.

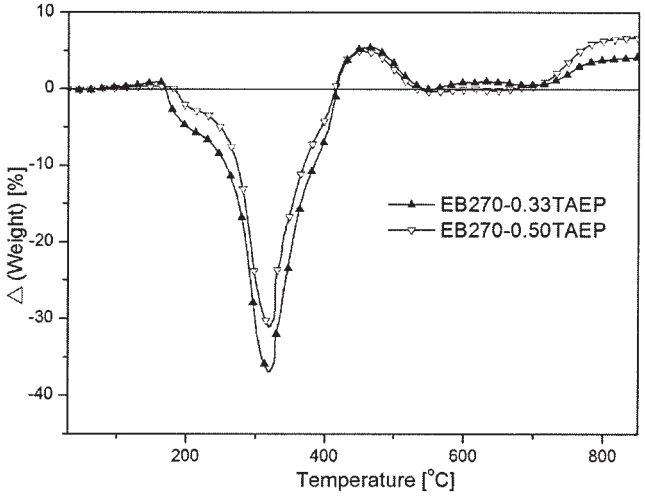

Figure 2 Weight difference curves of EB270/TAEP blends.

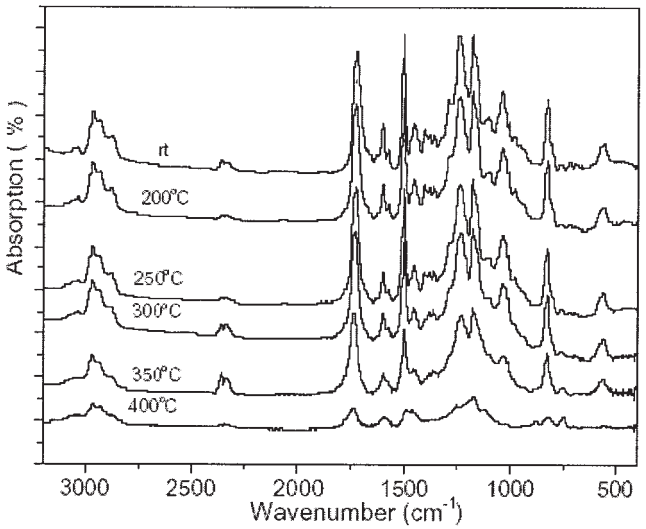

Figure 3 FTIR spectra of EB600 film during the thermal degradation in the range of RT −400°C.

Chemical structures changes during thermal degradation

Figure 3 shows the FTIR spectra of residual products after the degradation of EB600 at different temperatures. The samples gave little changes in the FTIR spectra before being heated to 300°C. The absorption at 1170 and 1260 cm^{-1} for ester group is still rather strong at 350°C. No new absorption bands are found during the thermal degradation up to 400°C. The FTIR spectra of residual products after degradation at different temperatures for EB600–0.33TAEP are shown in Figure 4. The absorption peaks at 1038 and 980 cm^{-1} for P—O—C decrease quickly with the increasing temperature and then disappeared at 300°C. On the other hand, the band at 2850–2980 cm^{-1} and the peak at 1723 cm^{-1} corresponding to C—H and C═O absorption, respectively, remain unchanged before 250°C. These results indicate that the degradation of EB600/TAEP blend before 250°C mainly proceeds via the destruction of P—O—C groups in the film. Compared with those in EB600, the absorption peaks at 2850–2980 cm^{-1} (C—H) and at 1723 cm^{-1} (C═O) decrease more quickly with the increasing temperature. However, some new absorption peaks in the FTIR spectra of residual products from EB600/TAEP blend appear simultaneously. The absorption peaks at 1150 and 1018 cm^{-1} might be assigned to the stretching vibration of P—O—C and PO_2/PO_3, respectively, as phosphate–carbon complexes.[17] The peaks at 1086 and 889 cm^{-1} might be attributed to the symmetric and asymmetric stretching vibration of P—O—P band.[18,19] Moreover, the peaks at 1300 cm^{-1} might be assigned to P═O absorption. These new peaks are rather strong even for the sample obtained from the degradation at 400°C. These evidences suggest that there is a difference in the thermal degradation mechanisms of EB600 and its blend with TAEP. P—O—C groups in the blend degrade at lower temperature to form poly(phosphoric acid), which catalyzes the degradation of EB600, and then reacts with the decomposition products of EB600, resulting in the decrease of flammable volatile compounds and promotion the formation of crosslinked char at higher temperature. These results indicate that the first negative peak in the weight difference curves of EB600/TAEP blends about 230°C can be attributed to the degradation of phosphate, and the second negative peak about 330°C can be attributed to the catalysis of poly(phosphoric acid).

Figure 5 shows the FTIR spectra of residual products after the degradation of EB270. The samples gave little changes in the FTIR spectra before being heated to 250°C, and then gave quickly changes over 250°C. The band about 1730 cm^{-1} attributed to C═O group of urethane and ester bonds quickly decreases from 250°C and almost disappear above 320°C. No new absorption bands are found during the thermal degradation period. The FTIR spectra of residual products for EB270–0.33TAEP are shown in Figure 6. It can also be seen that the P—O—C absorption at 1038 and 980 cm^{-1} decreases quickly with increasing temperature and then disappeared at 270°C. Moreover, those new peaks as mentioned earlier (EB600–0.33TAEP; FTIR spectra) also appear, which indicates that the complex phosphorus–carbon char are also formed at higher temperature for EB270–0.33TAEP. However, phosphate group, C═O group in urethane and ester bonds degrade almost simultaneously, which quickly decreased from 250°C and almost disappeared above 320°C. Thus, phosphate could not completely degrade

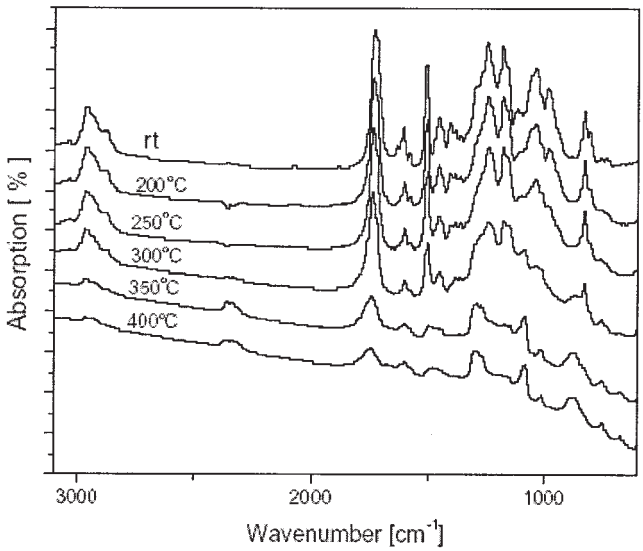

Figure 4 FTIR spectra of EB600–0.33TAEP film during the thermal degradation in the range of RT −400°C.

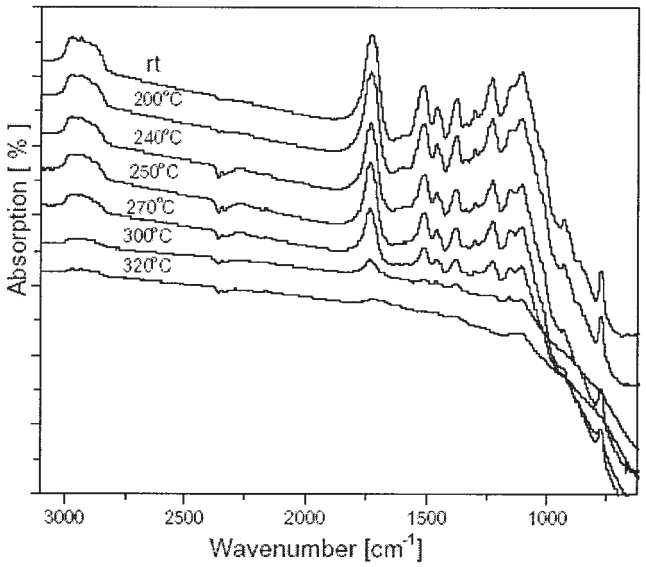

Figure 5 FTIR spectra of EB270 film during the thermal degradation in the range of RT −320°C.

to form poly(phosphoric acid) before the degradation of urethane and ester function. As a result, the interaction between of the degradation of EB270 and TAEP are not effective. However, phosphate completely degraded before the degradation of EB600, which began to degrade about 300°C, and thus the interaction was effective. Both EB270–0.33TAEP and EB270–0.50TAEP show large negative peaks about 320°C, with very small thermally stable peaks (about 5%) over 400°C in the weight difference curves. EB600–0.33TAEP and EB600–0.50TAEP show smaller negative peaks about 330°C with larger stabilization peaks about 25 and 10%, respectively.

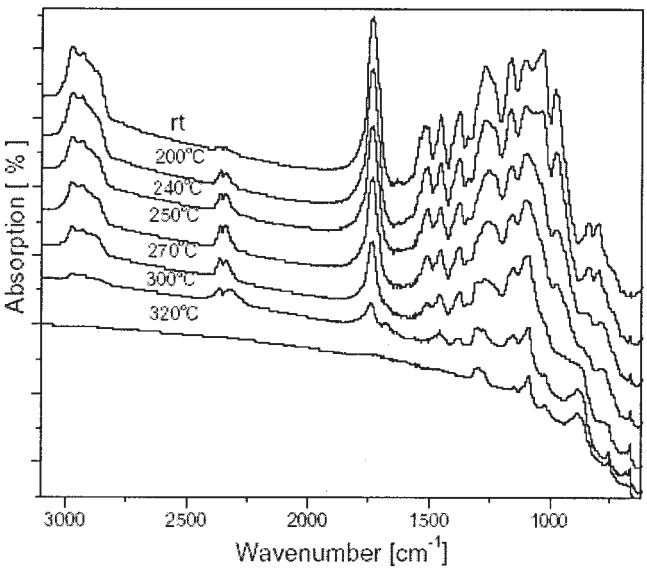

Figure 6 FTIR spectra of EB270–0.33TAEP film during the thermal degradation in the range of RT −320°C.

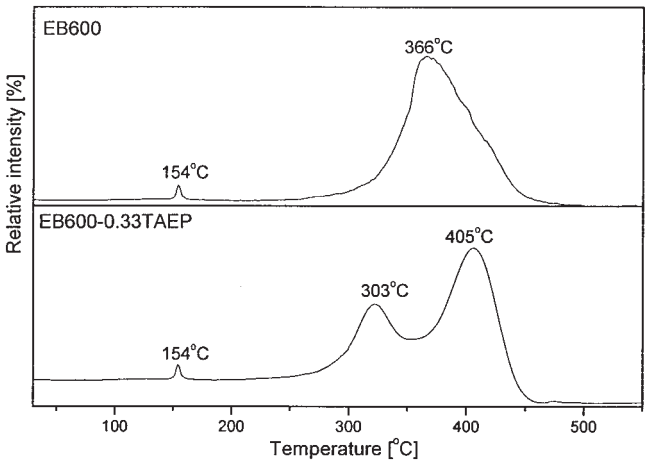

Figure 7 TIC curves of the decomposition processes of EB600 and EB600–0.33TAEP films.

Figure 7 shows the total ion current (TIC) chromatograms by DP–MS for the cured EB600 and EB600–0.33TAEP films. It can be observed that EB600 film has two peaks at 154 and 366 °C, whereas EB600–0.33TAEP film has three peaks at 154, 303, and 405°C. The mass spectra corresponding to the TICs at different temperatures are presented in Figure 8.

EB600 and EB600–0.33TAEP films at 154°C have the same mass spectra. The peaks at 105.0345 and 59.0510 *m/z* correspond to C_6H_5CO and $(CH_3)_2C(OH)$, respectively, which are the decomposition products of photoinitiator Darocur 1173. These are similar to the DP–MS results of TAEP in our previous work.[14] Therefore, these small peaks in the spectra of both polymers are mostly due to the volatilization of the photoinitiator.

In the mass spectra of EB600 film at 366°C (Fig. 8), the peaks at 356.1591 *m/z* for HO—Ar—$C(CH_3)_2$—Ar—O—$CH_2CH(OH)$—CH_2—OC(O) —CH═CH_2 and at 263.9820 *m/z* for CH_2═CH—Ar—O— $CH_2CH(OH)$—CH_2—OC(O)—CH═CH_2 appear. These structures are for the degradation products of the polyacrylate main chain. Therefore, the products at 366°C for EB600 film mainly result from the degradation of the main chain. In the mass spectra of EB600–0.33TAEP at 303 and 405°C(Fig. 8), the peak at 356.1591 *m/z* for HO—Ar—$C(CH_3)_2$—Ar—O— $CH_2CH(OH)$—CH_2—OC(O)—CH═CH_2 does not appear and the peak at 263.9820 *m/z* for CH_2═CH— Ar—O—$CH_2CH(OH)$—CH_2—OC(O)—CH═CH_2 is very small. Moreover, the peak at 43.9923 *m/z* for CO_2 becomes larger. The main peaks are about 254.1255 *m/z* for HO—Ar—$C^+(CH_3)$—Ar—O—CH_2—CH═CH_2 and 213.0876 *m/z* for HO—Ar—$C^+(CH_3)$—Ar—OH, respectively. Thus, the degradation of EB600–0.33TAEP is mainly due to the degradation of the ester groups. In our previous work, the degradation of TAEP has also been investigated by DP–MS. The results showed that phosphate

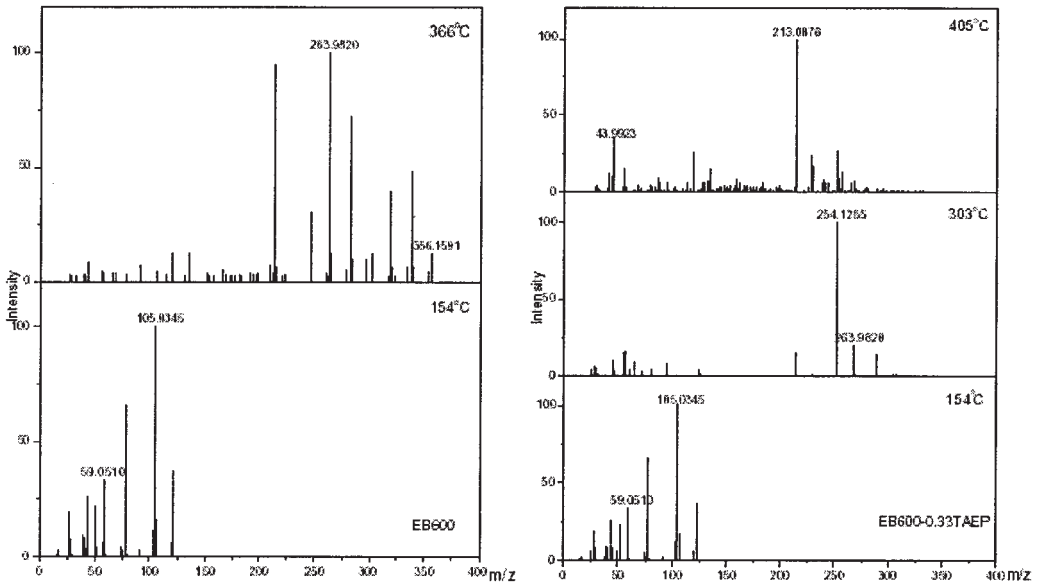

Figure 8 EI MS spectra of compounds evolved from EB600 and EB600–0.33TAEP films at different temperatures.

groups in TAEP first degraded to form poly(phosphoric acid) about 300°C[14] that further catalyzed the degradation of ester group and thus changed the degradation mode of EB600.

Figure 9 shows the TIC chromatograms by DP–MS for the cured EB270 and EB270–0.33TAEP films. It can be observed that EB270 film has three peaks at 80, 287, and 385°C, whereas EB270–0.33TAEP film has three peaks at 120, 292, and 440°C. The mass spectra corresponding to the TICs at different temperatures are presented in Figure 10.

It can also be seen that EB270 film at 80°C and Eb270–0.33TAEP film at 120°C have the same mass spectra, which are also exactly similar with the spectra of EB600 and EB600–0.33TAEP. Therefore, these small peaks in the spectra of both polymers are also due to the volatilization of the photoinitiator.

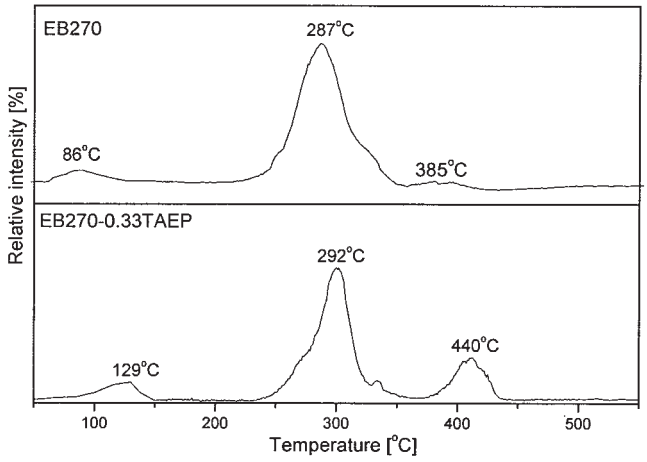

Figure 9 TIC curves of the decomposition processes of EB270 and EBb270–0.33TAEP films.

In the mass spectrum of EB270 at 287°C (Fig. 10), the peaks at 290.2166, 232.1699, 174.1254, and 116.0823 *m/z* correspond to $(C_3H_6O)_n$, n = 5, 4, 3, and 2, respectively. The peak at 58.0441 *m/z* corresponds to C_3H_6O. The peaks at 156.1184, 98.0748, and 42.0187 *m/z* correspond to $CH_2{=}CH{-}CH_2{-}O{-}(C_3H_6O)_2H$, $CH_2{=}CH{-}CH_2{-}O{-}CH_2{-}CH{=}CH_2$, and $CH_2{=}CH{-}CH_3$, respectively. The peak at 43.9923 *m/z* corresponds to CO_2. The literature has reported the thermal degradation of polyurethane.[20] Three general trends have been observed:

Depolymerization:

$$R{-}NH{-}C(O){-}O{-}R^{\cdot} \quad R{-}N{=}C{=}O + R^{\cdot}{-}OH$$

Primary amine formation:

$$R{-}NH{-}C(O){-}O{-}CH_2{-}CH_2{-}R^{\cdot} \rightarrow R{-}NH_2 + CO_2 + CH_2{=}CH{-}R^{\cdot}$$

Secondary amine formation:

$$R{-}NH{-}C(O){-}O{-}R^{\cdot} \rightarrow R{-}NH{-}R^{\cdot} + CO_2$$

Therefore, these peaks in the mass spectrum of EB270 at 287°C can be assigned to the products of depolymerization and primary amine formation trends of urethane structures. This indicates that the degradation of EB270 film at this stage can be attributed to the degradation of urethane structure.

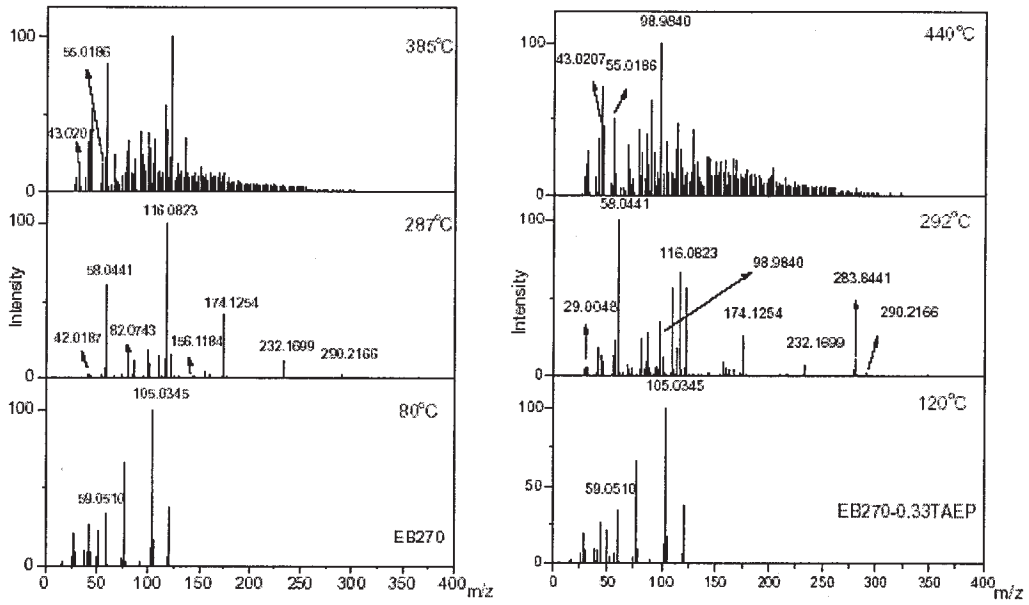

Figure 10 EI MS spectra of compounds evolved from EB270 and EB270–0.33TAEP films at different temperatures.

All the peaks in the mass spectrum of EB270 at 287°C also appear in the mass spectrum of EB270–0.33TAEP at 292°C (Fig. 10). However, the peaks at low molecular weight region become larger. The highest peak decreases from 116.0823 for EB270 to 58.0441 *m/z* for EB270–0.33TAEP. Moreover, some new peaks at 283.8441, 98.9840, 82.9906, and 64.9797 *m/z* corresponding to P_4O_{10}, H_4O_4P, H_4O_3P, and H_2O_2P, respectively, appear. These can be assigned to the degradation of phosphate groups, and has been investigated in our previous work.[14] Therefore, the degradation processes of both urethane and phosphate structures took place simultaneously, which is similar to the results from *in situ* FTIR measurements. The movement of the highest peak in the mass spectra indicates that phosphorus acid catalyzes the degradation of urethane to form smaller volatiles. Another new peak at 29.0048 *m/z* corresponds to CHO, the product of degradation of ester catalyzed by phosphorus acid, which has also been found during the degradation of TAEP in our previous work.[14] This also indicates the catalysis of phosphorus acid.

The mass spectra of EB270 film about 385°C and the EB270–0.33TAEP film about 440°C are very complex. The peaks about 116.0823 *m/z* for $(C_3H_6O)_2$ and 58.0441 *m/z* for C_3H_6O corresponding to the products of degradation of urethane structure are still the main peaks in the mass spectrum of EB270 at 385°C. Moreover, the peaks about 55.0186 *m/z* for $CH_2{=}CHC{=}O$ and 43.0207 *m/z* for $CH_2{=}CH{-}O$ corresponding to the degradation of polyarcylate main chain also appear. These indicate that this small peak for EB270 is mainly due to the degradation of remaining urethane structure and the main chain. However, the peak about 58.0441 *m/z* for C_3H_6O becomes very small in the mass spectrum of EB270–0.33TAEP at 440°C. This indicates that urethane structure has been almost completely degraded by the catalysis of phosphorus acid. The peak about 55.0186 *m/z* for $CH_2{=}CHC{=}O$ and 43.0207 *m/z* for $CH_2{=}CH{-}O$ corresponding to the degradation of polyarcylate main chain also appear. Thus, this peak of EB270–0.33TAEP is mainly due to degradation of the main chain.

Moreover, the peak about 98.9840 *m/z* for H_4O_4P appears in the mass spectrum of EB270–0.33TAEP at 440°C. Meanwhile, the peak for phosphorus acid is not found in the mass spectrum of EB600–0.33TAEP at 405°C. This result indicates that phosphorus acid can effectively react with the degradation products of EB600 to form char. However, it is not effective to react with the degradation products of EB270 to form char. As a result, TAEP are more efficient to improve the flame retardance of EB600 than that of EB270. The phosphorus-containing compounds as a family of condensed-phase FRs should first degrade to form phosphorus acids, which are able to increase the conversion of organic matter to char during burning. However, both the degradation of urethane structure of EB270 and the phosphate group of TAEP occur simultaneously, which determine that TAEP can not efficiently increase the conversion of EB270 to char. This is because the phosphate group can not effectively degrade to form poly(phosphoric acid), which can reactive with the degradation products of EB270 to form char, before the degradation of EB270. This result can also be approved by the former weight difference curves and CY during combustion and *in situ* FTIR measurements.

CONCLUSIONS

The flame retardance of epoxy acrylate EB600 and polyurethane acrylate EB270 can be improved by the addition of TAEP. Phosphate group in TAEP degrades first to form poly(phosphoric acid)s before the degradation of EB600, which are effective to catalyze the degradation of EB600 to form char. However, the degradation of phosphate group in TAEP occurs simultaneously with the degradation of EB270. As a result, the addition of TAEP can not effectively increase the conversion of EB270 to char. Thus, the addition of TAEP can more effectively improve the thermal stability, the flame retardance, and the CY during the combustion of EB600 than EB270.

References

1. Valet, A. Prog Org Coat 1999, 35, 223.
2. Maag, K.; Lenhard, W.; Löffles, H. Prog Org Coat 2000, 40, 93.
3. Chen-Yang, Y. W.; Chuang, J. R.; Yang, Y. C.; Li, C. Y.; Chiu, Y. S. J Appl Polym Sci 1998, 69, 115.
4. Ravey, M.; Pearce, E. M. J Appl Polym Sci 1997, 63, 47.
5. Inan, T. Y. Polym Prepr 1999, 40, 47.
6. Zhu, S. W.; Shi, W. F. Polym Degrad Stab 2003, 2, 233.
7. Avci, D.; Albayrak, A. Z. J Polym Sci Part A: Polym Chem 2003, 41, 2207.
8. Kracklauer, J. In Flame-Retardant Polymeric Materials; Lewin, M.; Atlas, S. M.; Pearce, E. M., Eds.; Plenum Press: New York, 1978; Vol. 2, p 285.
9. Randoux, T.; Vanovervelt, J. C.; Van den Bergen, H.; Camino, G. Prog Org Coat 2002, 45, 281.
10. Guo, W. J. J Polym Sci Part A: Polym Chem 1992, 30, 819.
11. Banks, M.; Ebdon, J. R.; Johnson, M. Polymer 1994, 34, 4547.
12. Cullis, C.; Hirschler, M. M. The Combustion of Organic Polymers. Clarendon Press: Oxford, 1981; p 241.
13. Nair, C. P. R.; Clouet, G.; Guilbert, Y. Polym Degrad Stab 1989, 26, 305.
14. Liang, H. B.; Shi, W. F. Polym Degrad Stab 2004, 84, 525.
15. Liang, H. B.; Shi, W. F. J Appl Polym Sci 2005, 97, 185.
16. Giraud, S.; Bourbigot, S.; Rochery, M.; Vroman, I.; Tighzert, L.; Delobel, R. Polym Degrad Stab 2002, 77, 285.
17. Bourbigot, S.; Bras, M. L.; Delobel, R.; Trémillon, J. M. J Chem Soc Faraday Trans 1996, 92, 3435.
18. Bugajny, M.; Le Bras, M.; Bourbigot, S.; Delobel, R. Polym Int 1999, 48, 264.
19. Le Bras, M.; Bourbigot, S.; Revel, B. J Mater Sci 1999, 34, 5777.
20. Boutin, M.; Lesage, J.; Ostiguy, C.; Bertrand, M. J. J Anal Appl Pyrolysis 2003, 70, 505.